Intramolecular Electron Transfer on the Vibrational Timescale and Rate Constants Estimated by IR Absorption Band Shape Analysis

Tasuku Ito,[a,*] Tadashi Yamaguchi,[a] Clifford P. Kubiak[b]

[a] Graduate School of Science, Tohoku University, Sendai 980-8578, Japan
[b] Department of Chemistry and Biochemistry, University of California, San Diego, La Jolla, CA 92093-0358, U.S.A.

SUMMARY: From electrochemical studies, the thermodynamic stability of the mixed valence (one electron reduced) state and the electronic coupling between linked Ru_3 units, was studied in the series of the ligand bridged hexaruthenium clusters, $[Ru_3(\mu_3\text{-}O)(\mu\text{-}CH_3CO_2)_6(CO)(L)(\mu\text{-}BL)Ru_3(\mu_3\text{-}O)(\mu\text{-}CH_3CO_2)_6(CO)(L)]$ (BL = pyrazine: L = 4-dimethyl-aminopyridine (dmap) (**1a**), pyridine (py) (**1b**), 4-cyanopyridine (cpy) (**1c**), 1-azabicyclo[2.2.2]octane (**1d**); BL = 4,4'-bipyridine: L = dmap (**2a**), py (**2b**), cpy (**2c**); BL = 2,7-diazapyrene: L = dmap (**3a**); BL = 1,4-diazabicyclo-[2.2.2]octane: L = dmap (**4a**), py (**4b**), cpy (**4c**)). The mixed valence states undergoing the most rapid intramolecular electron transfers were observed by reflectance IR spectroelectrochemistry. By simulating dynamical effects on the observed ν(CO) absorption bandshapes, the rate constants, k_e, for electron transfer in the mixed valence states of **1a**, **1b**, **1c** and **1d** were estimated to be 9×10^{11} s^{-1} (at room temperature (rt)), 5×10^{11} s^{-1} (at rt), *ca.* 1×10^{11} s^{-1} (at rt), and 1×10^{12} s^{-1} (at -18 °C), respectively. The rate constant for the -1 mixed valence state of **2a** is close to the lower limit that can be estimated by this approach, between 1×10^{10} and 1×10^{11} s^{-1}.

Introduction

Spectroscopic techniques for molecular structure determination have their own timescales. As is well known, spectral coalescence in nuclear magnetic resonance (NMR) is related to the lifetime of a chemical species in solution. The intrinsic timescale of NMR is on the order of milliseconds. In infrared (IR) spectroscopy, the timescale is on the order of picoseconds. Intramolecular processes such as electron and energy transfer can occur on the picosecond timescale, and there is a possibility that fast processes such as these could cause infrared spectral coalescence. We recently reported our observations of coalescence of the C-O stretching bands of carbon monoxide (ν(CO)) ligands in the most rapidly exchanging mixed valence complexes of hexanuclear ruthenium clusters.[1,2] The mixed valence complexes are one-electron reduced species of ligand bridged dimers of triruthenium clusters of the type, $[Ru_3(\mu_3\text{-}O)(\mu\text{-}CH_3CO_2)_6(CO)(L)(\mu\text{-}BL)Ru_3(\mu_3\text{-}O)(\mu\text{-}CH_3CO_2)_6(CO)(L)]$ shown in Fig. 1, where BL denotes bridging ligand. In the neutral isolated states of all the compounds, each

 CCC 1022-1360/00/$ 17.50+.50/0

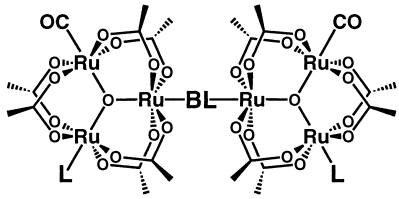

BL \ L	(dmap)	(py)	(cpy)	(abco)
(pz)	**1a**	**1b**	**1c**	**1d**
(bpy)	**2a**	**2b**	**2c**	—
(dap)	**3a**	—	—	—
(dabco)	**4a**	**4b**	**4c**	—

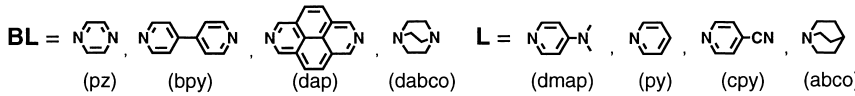

Fig. 1: Structure of $[Ru_3(\mu_3\text{-}O)(\mu\text{-}CH_3CO_2)_6(CO)(L)(\mu\text{-}BL)Ru_3(\mu_3\text{-}O)(\mu\text{-}CH_3CO_2)_6(CO)(L)]$ and numbering of the compounds. pz = 1,4-pyrazine, bpy = 1,4-bipyridine, dap = 2,7-diazapyrene, dabco = 1,4-diazabicyclo[2.2.2]octane, abco = 1-azabicyclo-[2.2.2]octane.

trinuclear Ru_3 unit formally contains one Ru(II) and two Ru(III) centers and the carbonyl ligand is coordinated to the formally divalent center. In this paper, we report the unusual characteristics of the IR spectra of **1a-1d** and **2a-2b** along with electrochemical data of all the compounds in Fig. 1.

Electrochemically Generated Mixed Valence States and Their Thermodynamic Stabilities

Figure 2 shows cyclic voltammograms (CV) of a series of Ru_3 dimes where the bridging ligand is fixed to pyrazine and the terminal ligands are varied. Figure 3 shows CV's of a series of Ru_3 dimes where the bridging ligand is varied and the terminal ligand is fixed to dmap. In all the CV's in Figs. 3 and 4, two-electron oxidation waves are observed at approximately $E_{1/2}(+2/0)$ = +0.50 and $E_{1/2}(+4/+2)$ = +1.3 V vs. SSCE. Here, the overall charges of the complexes are expressed in parentheses. On the other hand, each compound generally displays *two single electron reduction waves* that correspond formally to $Ru_3^{III,III,II}$-BL-$Ru_3^{III,III,II}$/$Ru_3^{III,III,II}$-BL-$Ru_3^{III,II,II}$ (0/-1) and then $Ru_3^{III,III,II}$-BL-$Ru_3^{III,II,II}$/$Ru_3^{III,II,II}$-BL-$Ru_3^{III,II,II}$ (-1/-2). In the case of **4a**, the splitting between the (0/-1) and (-1/-2) states is too small ($\Delta E \approx 0$ mV) to resolve by cyclic voltammetry. One important contribution to the magnitude of the splitting between the single electron (0/-1) and (-1/-2) reduction waves, ΔE, is the stabilization energy imparted to the -1 state by electron delocalization. Comproportionation constants, K_c = exp ($\Delta EF/RT$), estimated from ΔE are also given in Figs. 3 and 4. The mixed valence species, i.e., the -1 state exists in the region of ΔE between the (0/-1) and (-1/-2) waves and the magnitude of ΔE, and thereby K_c, reflects stability of the mixed valence state. Redox potential data for the (0/-1) and (-1/-2) processes are summarized in Table 1.

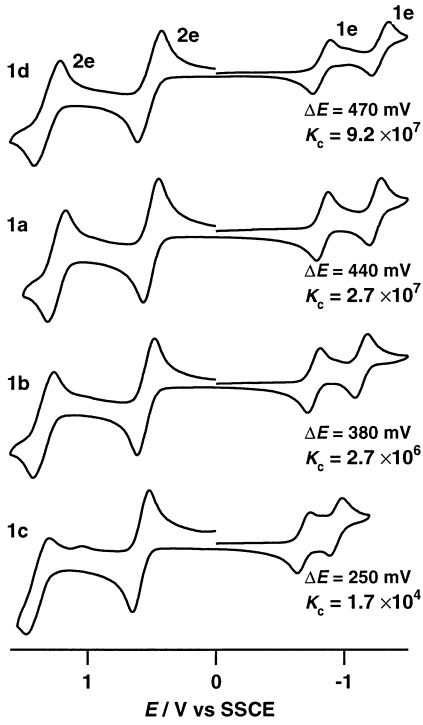

Fig. 2: Cyclic voltammograms, ΔE, and K_c of [{$Ru_3(\mu_3\text{-}O)(\mu\text{-}CH_3CO_2)_6(CO)(L)$}$_2(\mu$-pz)] (L = abco (**1d**), dmap (**1a**), py (**1b**), cpy (**1c**)).

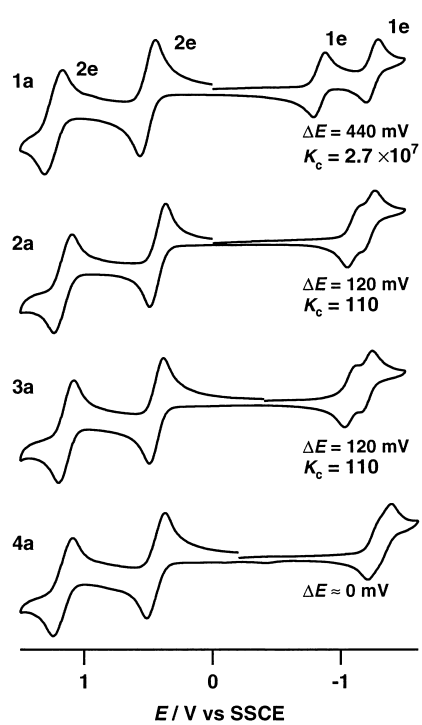

Fig. 3: Cyclic voltammograms, ΔE, and K_c of [{$Ru_3(\mu_3\text{-}O)(\mu\text{-}CH_3CO_2)_6(CO)(dmap)$}$_2(\mu$-BL)] (BL = pz (**1a**), bpy (**2a**), dap (**3a**), dabco (**4a**)).

An interesting aspect of these complexes is that the splitting, ΔE, depends strongly on the ancillary ligands (dmap, py, cpy, abco) and on the bridging ligands (pz, bpy, dap, dabco). Thus, as the adjustable pyridyl ligand in the series **1a**-**1c** and **2a**-**2c** is changed from dmap in **1a** and **2a** to an unsubstituted pyridine for **1b** and **2b** to an electron withdrawing cpy for **1c** and **2c**, the values of ΔE and K_c decrease considerably (Table 1). Compound **1d** with abco, which has the largest pK_a of 11.1 among the present series of terminal ligands, possesses the largest ΔE and K_c.[3] The bridging ligand π-electron systems mediate electronic coupling between the two Ru_3 centers, and the overlap between the Ru_3 cluster dπ-electron system and the bridging ligand π^* system appears to be very favorable. In fact, the dabco bridged compound **4a**, which has no π-electron system in the bridging ligand, shows essentially no electronic coupling ($\Delta E \approx 0$). The relevant Ru d level is closer to the pz π^* level in **1a** than it is in **1c**, and closer to the bpy π^* level in **2a** than it is in **2c**. This description of the electronic structure is supported by experimental evidence.[2] In general, electronic coupling falls off exponentially with increasing distance between electronically interacting centers. The center to

Table 1. Electrochemical Data for [{$Ru_3(\mu_3\text{-}O)(\mu\text{-}CH_3CO_2)_6(CO)(L)\}_2(\mu\text{-}BL)$]

	BL	L	$E_{1/2}(0/-1)$[a], V	$E_{1/2}(-1/-2)$[a], V	ΔE (mV)	K_c
1a	pz	dmap	-0.89	-1.33	440	2.7×10^7
1b	pz	py	-0.81	-1.19	380	2.7×10^6
1c	pz	cpy	-0.68	-0.93	250	1.7×10^4
1d	pz	abco	-0.84	-1.31	470	9.2×10^7
2a	bpy	dmap	-1.11	-1.23	120	1.1×10^2
2b	bpy	py	-1.03	-1.11	80	2.3×10^1
2c	bpy	cpy	-0.91(2e)		≈ 0	< 10
3a	dap	dmap	-1.08	-1.20	120	1.1×10^2
4a	dabco	dmap	-1.25	-1.31	60	3×10^1
4b	dabco	py	-1.12	-1.17	50	7×10^0
4c	dabco	cpy	-0.94(2e)		≈ 0	< 10

[a] Cyclic voltammograms recorded in 0.1 M tetra-n-butylammonium hexafluorophosphate in dichloromethane, V versus saturated sodium chloride calomel electrode (SSCE).

center separation between Ru_3O units in the crystal structure of **1a** is 10.9 Å,[4] and it is estimated at ca. 15.3 Å in bpy bridged complexes. The longer separation between Ru_3 centers in **2a**-**2c** and **3a** decreases the intercluster electronic coupling, thereby decreasing ΔE values.

IR Spectra of the Mixed Valence Species in the ν(CO) Region

The vibrational spectra of complexes **1a**-**1d** and **2a**-**2c** were obtained by using reflectance IR spectroelectrochemistry (SEC). Controlled potentials were applied to prepare the singly (-1) and doubly (-2) reduced states of cluster for IR spectroscopic observation. Measurements were carried out at room temperature unless otherwise stated. Experiments on **1d** were carried out at -18 °C, because reduced species (the -1 and -2 states) of this compound were unstable at room temperature. Figures 4(a) and 4(b) show IR spectra in the ν(CO) region of pyrazine bridged complexes **1a**-**1d** and 4,4'-bipyridine bridged complexes **2a**-**2b**, respectively. Let us discuss first the pyrazine bridged systems, **1a**-**1d**. In the isolated (0) state, **1d** exhibits a single ν(CO) band at 1937 cm^{-1} (Fig. 4(a) top), indicating that two Ru_3 units in **1d** are pairwise equivalent. The doubly reduced species also gives rise to a single ν(CO) band, but at 1890 cm^{-1}, reflecting identical re·lox states at each $Ru_3^{III,II,II}$ cluster. Complexes **1a**-**1c** similarly exhibit single ν(CO) bands in the neutral state and -2 state, respectively. Interestingly, however, the single electron reduced state of **1d** shows a broad absorption band at the average energy of the bands observed for the neutral (0) and doubly reduced (-2) states of **1d** (Fig. 4(a) top). The degree of "coalescence" of the IR spectra depends on the degree of electronic coupling between the

pyrazine-linked Ru_3 clusters (Fig. 4a). As ΔE (or K_c) decreases from 470 mV (9.2×10^7) for **1d** to 250 mV (1.7×10^4) for **1c**, two distinct ν(CO) bands at 1931 cm^{-1} and 1904 cm^{-1} become resolved for **1c**. Cluster **1b** with an intermediate value of ΔE (K_c) of 380 mV (2.7×10^6) shows an intermediate degree of spectral "coalescence" in the singly reduced state.

Similarly, both the neutral and -2 states of the bpy bridged complexes **2a**-**2c** exhibit one sharp ν(CO) band in the IR (Fig. 4(b)). The spectra of the -1 states of **2a** and **2b** consist of two well-resolved and well-separated ν(CO) bands, perturbed only slightly relative to the spectra of the neutral and -2 states. Careful analysis for **2a** suggests that a small amount of broadening may be occurring (vide infra). For **2c**, a reliable spectrum of the -1 state could not be obtained due to < 50 mV separation between the (0/-1) and (-1/-2) CV waves. In clusters **2a**-**2c** the electronic coupling is small as evidenced by cyclic voltammetry. Overall, the singly reduced states of **2a**-**2c** can be viewed as valence trapped or localized compounds.

The IR spectral feature in the ν(CO) region of the -1 mixed valence state is very different

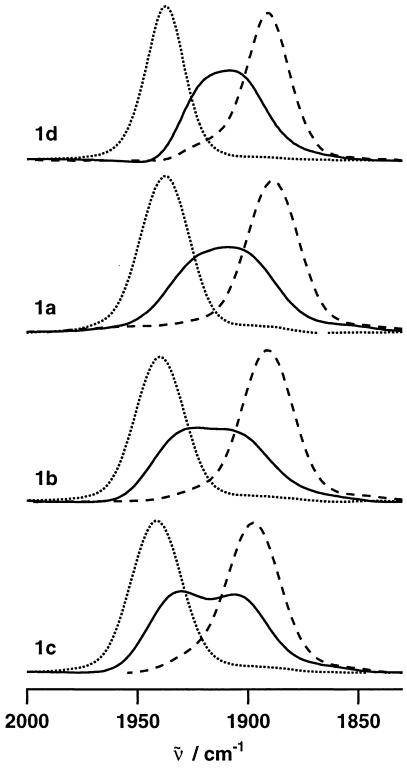

Fig. 4(a): IR spectra in the ν(CO) region for $[\{Ru_3(\mu_3\text{-}O)(\mu\text{-}CH_3CO_2)_6(CO)(L)\}_2(\mu\text{-}pz)]^{n+}$ (n = 0 (···), -1 (—), -2 (- - -)) for L = abco (**1d**), dmap (**1a**), py (**1b**), cpy (**1c**).

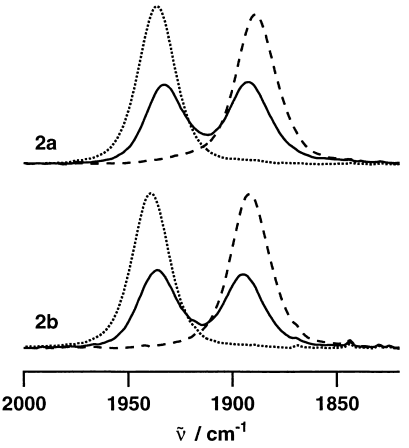

Fig. 4(b) :IR spectra in the ν(CO) region for $[\{Ru_3(\mu_3\text{-}O)(\mu\text{-}CH_3CO_2)_6(CO)(L)\}_2(\mu\text{-}bpy)]^{n+}$ (n = 0 (···), -1 (—), -2 (- - -)) for L = dmap (**2a**), py (**2b**).

between pyrazine bridged complexes **1a**-**1d** and 1,4-bipyridine complexes **2a**-**2c**. The vast difference in spectral characteristics arises from the electronic interactions between two Ru_3 units through the bridging ligand, as is seen in their electrochemical behavior. The use of longer bpy bridges in **2a**-**2c** attenuates electronic coupling to the point that in **2c** the -1 charge transfer state is no longer defined. Preliminary experiments show essentially no temperature dependence of the IR spectra in the range from room temperature down to -40°C.

Estimation of Rate Constants of Intramolecular Electron Transfer in the Mixed Valence State

At the present time, we have no evidence of a process other than intramolecular electron transfer to account for the changes observed in the IR spectral line shapes of our systems. We carried out the Bloch equation type analysis for the IR line broadening which is developed by McClung.[5]. Figure 5 shows an example of tne simulated spectral line shapes as a function of rate constant k_e and a comparison to the observed spectrum of **1d**$^-$. Similar analyses were carried out for **1a**$^-$ - **1c**$^-$ and **2a**$^-$.[2)] The rate constants k_e of electron transfer estimated by this type of simulation for **1d**$^-$, **1a**$^-$, **1b**$^-$, and **1c**$^-$ are (10 ± 2) × 10^{11} at -18 °C, (9 ± 3) × 10^{11}, (5 ± 3) × 10^{11}, ca. 1 × 10^{11} s^{-1}, respectively. Simulated spectra as a function of k_e for **1c**$^-$ shows that k_e for **1c**$^-$ is close to the lower limit that can be determined reliably by this approach.[2)] Simulation for the IR spectrum of **2a**$^-$ suggests that k_e for **2a**$^-$ could be faster than 1 × 10^{10} s^{-1}.

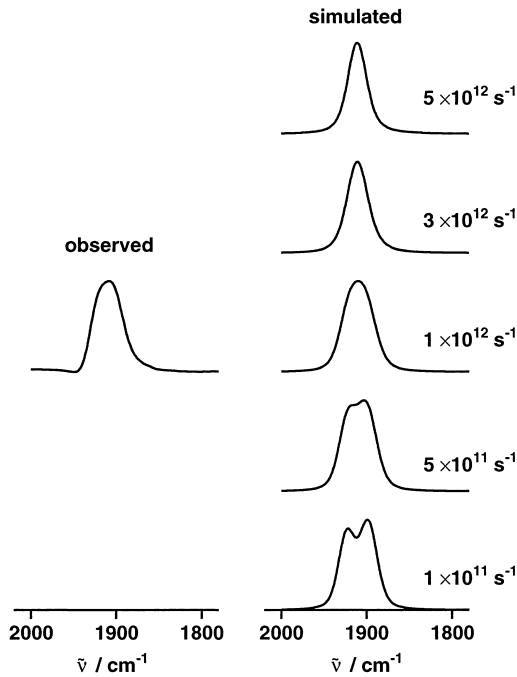

Fig. 5: Comparison of observed to simulated infrared spectra in the ν(CO) region for **1d**$^-$ as a function of the intramolecular electron transfer rate constant, k_e.

Conclusions

There are uncertainties in the rates of electron transfer estimated by Bloch equation simulation of the IR band shape. The precise relationship between IR line shape and electron-transfer dynamics still needs to be refined. But IR band coalescence phenomena observed in this study suggest that intramolecular electron transfer does occur on the IR timescale and offers great advantages for comparing theory and experiment. The present results suggest that the pyrazine bridged linear oligomer of the Ru_3 cluster shown below should be a conducting polymer in the reduced state. Thus far, Ru_3 tetramer has been prepared using the synthetic method of stepwise elongation of a Ru_3 unit.[6)]

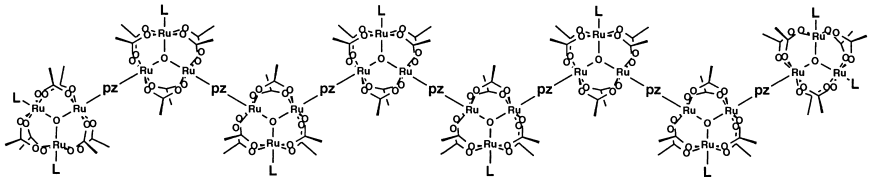

Acknowledgment

This work was supported by Grants-in-Aid for Scientific Research (Priority Areas No. 10149102 "Metal-assembled Complexes") and for International Scientific Research (Joint Research No. 11694051) from the Ministry of Education, Science, and Culture, Japan. We also thank collaborators given in the references.

References

1. T. Ito, T. Hamaguchi, H. Nagino, T. Yamaguchi, J. Washington, C. P. Kubiak, *Science* **277**, 660 (1997).
2. T. Ito, T. Hamaguchi, H. Nagino, T. Yamaguchi, H. Kido, I .S. Zavarine, T. Richmond, J. Washington, C. P. Kubiak, *J. Am. Chem. Soc.* **121**, 4625 (1999)
3. T. Yamaguchi, N. Imai, T. Ito, C. P. Kubiak, Details of the study on **1d** will be reported elsewhere.
4. umpublised result.
5. F.-W Grevels, K. Kerpen, W. E. Klotzbucher, R. E. D. McClung, G. Russel, M. Viotte, K. Schaffner, *J. Am. Chem. Soc.* **120**, 10423 (1998)
6. H. Kido, H. Nagino, T. Ito, *Chem. Lett.* 745 (1996)